Proceedings, 11th International Conference on Clouds & Precipitation
Montreal, CANADA, **2**,
Aug. 17-21, 1992, 719-722.

A NUMERICAL STUDY OF THE MOMENTUM BUDGET OF A SQUALL LINE

Ming-Jen Yang and Robert A. Houze, Jr.

Department of Atmospheric Sciences
University of Washington, AK-40
Seattle, Washington 98195

1. INTRODUCTION

Mesoscale budget studies are useful in determining the interaction between a mesoscale convective system (MCS) and its environment. Studies of the momentum transport by lines of convection in the tropics (LeMone 1983; LeMone *et al.* 1984) and midlatitudes (Gao *et al.* 1990) have shown that the momentum transport is generally countergradient in the normal-line direction and downgradient in the along-line direction.

A typical structure for a squall-line MCS is leading-edge convection followed by a horizontally uniform stratiform precipitation area (Zipser 1969; Houze 1977; Smull and Houze 1985). The momentum balance and transport within these two regions may be quite different. The objective of this study is to decompose the momentum budget and flux into processes associated with convective and stratiform regions of a midlatitude squall line. This study is based on a numerical simulation of the intense squall line that occurred on 10-11 June 1985 during the Oklahoma-Kansas Preliminary Regional Experiment for STORM-Central (called PRE-STORM for short; see Cunning 1986).

2. MODEL

The model used in this study is a two-dimensional version of the Klemp-Wilhelmson compressible cloud model (Klemp and Wilhelmson 1978; hereafter KW) which includes the cloud microphysical bulk parameterization as described by Lin *et al.* (1983). The basic-state environment is assumed constant in time and horizontally homogeneous. Large-scale motion, surface fluxes, and radiation are neglected. Stretched grids are used in both vertical and horizontal directions (similar to Fovell and Ogura 1988: hereafter FO) in order to optimize resolution. In the vertical, the grid size of the lowest layer is 140 m; the grid size of the highest layer is 550 m; and the model top is at 21.7 km. A total of 455 grid points are used in the horizontal. The central 315 points comprise a fine mesh with 1-km resolution, and the total horizontal domain size is thus 4,814 km. The top and bottom of the domain are rigid lids. Since sound waves exist in the compressible equations, a time-splitting scheme is used to provide numerical efficiency by treating sound wave modes (2 s time step) and cloud-scale gravity wave modes (6 s time step) separately.

The initial temperature and moisture profiles for the simulation were from the 2331 UTC 10 June sounding from Enid, Oklahoma (Fig. 1a). This sounding showed the environmental conditions 4 h before the squall line passed the station. The initial normal-line wind profile is in Fig. 1b. The convective available potential energy indicated by this sounding was 3,323 J kg^{-1}, higher than the average value for springtime severe storms in this region (Bluestein and Jain 1985). However, the wind shear is so strong that a model storm cannot survive if it is initiated with the observed wind profile. Therefore, a similar approach to that of Fovell and Ogura (1989) is taken, *i.e.*, a reduced shear (3×10^{-3} s^{-1} in the lowest 2.5 km, no shear above 2.5 km) is used to initiate the storm. Once the cold pool of the storm is strong enough to act against the wind shear (model time ~6 h), the background wind is slowly changed back to the observed profile. A 5°K thermal similar to that used by KW is put in the central domain to initiate convection. The thermal is centered at 1.4 km AGL with horizontal radius 10 km and vertical radius 1.4 km.

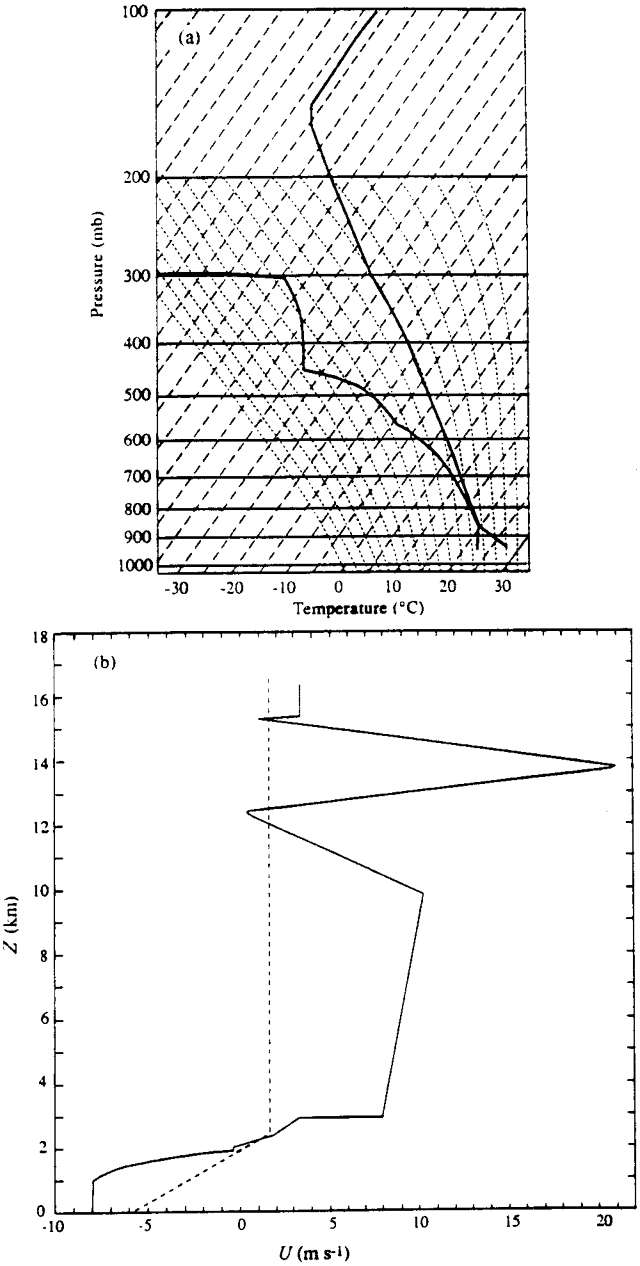

Fig. 1 Initial sounding used in the model simulations. (a) The temperature and dew-point temperature profiles (dark lines) are plotted in skew-T format. Curved lines are moist adiabats. (b) Observed line-normal wind profile is the solid line, and the reduced wind-shear profile used to initiate the storm is the dashed line.

Model verification shows that the cloud model can reproduce many realistic aspects of the squall line, which are known from observations (*e.g.*, Johnson and Hamilton 1988; Biggerstaff and Houze 1991). Specifically, the model simulated the storm-relative front-to-rear (FTR) flows in both upper and lower levels and the rear-to-front (RTF) flows in between (Fig. 2a), the upshear tilt of the updrafts (Fig. 2b), a precipitation-induced high at the gust front and a wake low (not shown), the leading convective rainfall followed by a transition zone, and the trailing stratiform precipitation. Thus, we proceed to an examination of the momentum budget of the model storm.

3. METHODOLOGY

Since the computational domain moves with the squall line so that the model storm is always in the fine mesh, the horizontal momentum equation used in the model is:

$$u'_t = -cu'_x - (u'u')_x - (\rho_o wu')_z / \rho_o - c_p \theta_{vo} \pi_x + D_{u'} \qquad (1)$$

where x and z are the horizontal and vertical coordinates. When used as subscripts, x and z denote partial derivatives. u' is the system-relative horizontal flow, c is the domain translation speed (usually the squall-line propagation speed), w is the vertical velocity, ρ_o is the basic-state density, c_p is the specific heat at constant pressure, θ_{vo} is the basic-state virtual potential temperature, π is the nondimensional pressure, and $D_{u'}$ is the sub-grid scale turbulence term (the detailed definition of each symbol is given in KW). From the model output, each term in (1) can be directly calculated.

In order to understand how each physical process contributes to the balance of the u-momentum equation during the lifetime of the model storm, three characteristic 30-min periods (at model times 376-406 min, 556-586 min, and 736-776 min) were chosen to represent the three stages of the storm: developing, mature, and decaying. Then each term in (1) is averaged over the 30-min period with a 2-min data interval. The reason for the time average is that an individual convective or precipitation cell has a regeneration time scale (~10 min) shorter than that of the convective and mesoscale structures in which we are most interested, and the small-scale structures associated with individual precipitation cells can be smoothed out by taking the time average over a period longer than that of the cell regeneration period (FO). In addition to the time average, a horizontal average was also taken of each term in (1) over two regions: one over the entire convective rainfall region, and the other over the whole stratiform precipitation region (the distinction between the convective and stratiform precipitation regions was based on the time-average surface rainfall rate).

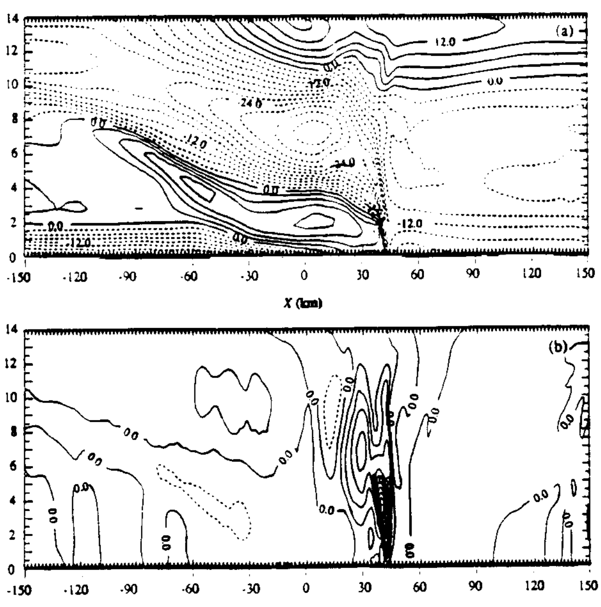

Fig. 2 Time-averaged wind fields at the mature stage (model time 556-586 min). (a) Horizontal storm-relative flow contoured every 3 m s^{-1} with negative values dashed. (b) Vertical flow contoured every 1 m s^{-1} with negative values dashed. The convective region is between x = 12 and 43 km, and the stratiform region is between x = −50 and 11 km. Storm motion is from left to right.

4. HORIZONTAL MOMENTUM BUDGET

In general, the vertical profiles for u momentum at the three life cycle stages are of a similar shape. The profiles differ mainly in their magnitudes and heights of their maxima and minima. Fig. 3a shows the vertical profiles for the terms in the u-momentum budget of the convective region during the mature stage. The horizontal pressure gradient produces FTR acceleration throughout the whole troposphere except at very low and high levels. Horizontal advection is roughly out of phase with vertical advection. Sub-grid scale turbulence is the smallest effect. The net acceleration is RTF in lower levels (below 4.5 km) and FTR above. The vertical profile of the u momentum in the stratiform region during the mature stage (Fig. 3b) is different from that in the convective region. The pressure gradient produces RTF acceleration throughout the entire troposphere except at lower levels (below 2 km). Horizontal advection oscillates in the vertical but is again strongly out of phase with vertical advection. Sub-grid scale turbulence is again the smallest term. The net acceleration is FTR in lower and upper levels, and RTF in between, which is consistent with the flow pattern in the stratiform region.

5. IMPACT OF MOMENTUM FLUX ON MEAN FLOW

In this section, we examine the effect of momentum transport on the horizontal (line-normal) mean flow in the convective and stratiform regions. Fig. 4a shows the area-averaged horizontal wind profiles in the convective region at the three life cycle stages, while Fig. 4b displays the corresponding mean momentum flux profiles. Consistent with the upshear tilting of the updraft and downdraft in the convective region, the momentum flux within the whole troposphere is negative during these three stages except in the midlevels at the mature stage. The direction of the vertical momentum transport is indicated by

$$\overline{u^* w^*} = -K \frac{\partial \overline{u'}}{\partial z} \qquad (2)$$

where

$$u' = \overline{u'} + u^*, w = \overline{w} + w^* \qquad (3)$$

In (2) and (3), the overbar denotes an area average, while the asterisk denotes the departure from the average. By the mixing length theory, $\overline{u^* w^*}$ is said to be downgradient if K is positive, and countergradient if K is negative. Fig. 4a and b shows that initially the momentum flux is mostly downgradient in the convective region, becomes more countergradient in the mature stage, and is mostly downgradient again in the decaying stage. Fig. 5 is the same as Fig. 4 except for the stratiform region, and the results inferred from it appear to be consistent with Gao *et al.* (1990). However, their 00 UTC profile was subject to large-scale environmental variation which is excluded in our study. In contrast to the result in the convective region, the momentum transport in the stratiform region is mostly countergradient at first and then becomes more and more downgradient as the system ages. The different momentum transport characteristics between convective and stratiform regions have not been indicated in previous studies. The reason for this difference will be explored by calculating the momentum flux from the model result for each region and each life cycle period. In this way, we shall isolate the main mechanism for the production of momentum flux of the indicated sign. This work is in progress.

6. CONCLUSION

In this study, we have examined the momentum budget of a numerical simulation of the 10-11 June 1985 squall line and separated the processes occurring in the convective region of the storm from those occurring in the stratiform region. In the *u*-momentum budget of the convective region, the pressure gradient produces FTR acceleration within the whole troposphere, except at very low and high levels. Horizontal advection is roughly out of phase with vertical advection. Sub-grid scale turbulence is the smallest effect. The net acceleration is RTF in lower levels (below 4.5 km) and FTR above. In the stratiform region, the pressure

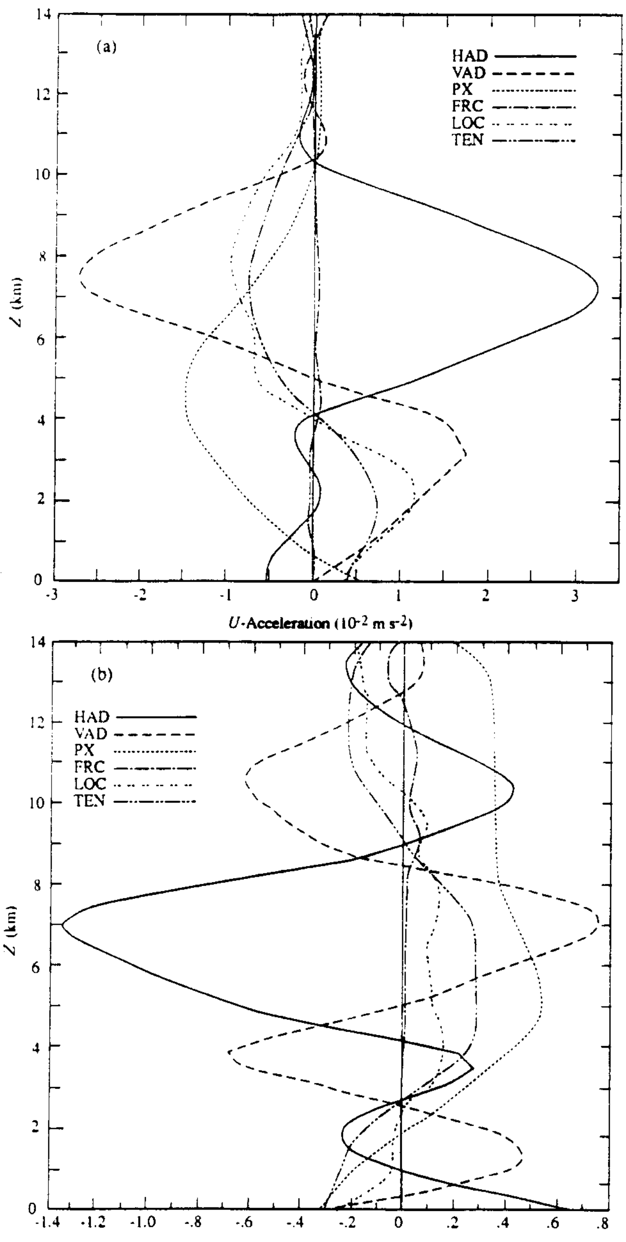

Fig. 3 The vertical profiles of each term in the u-momentum equation averaged over (a) the convective and (b) the stratiform region. LOC denotes the local time rate of change term (u'_t), TEN the apparent tendency term ($-cu'_x$), HAD the horizontal advection ($-(u'u')_x$), VAD the vertical advection ($-(\rho_o wu')_z/\rho_o$), PX the pressure gradient force ($c_p\theta_{vo}\pi_x$), and FRC the sub-grid scale turbulence ($D_{u'}$), respectively.

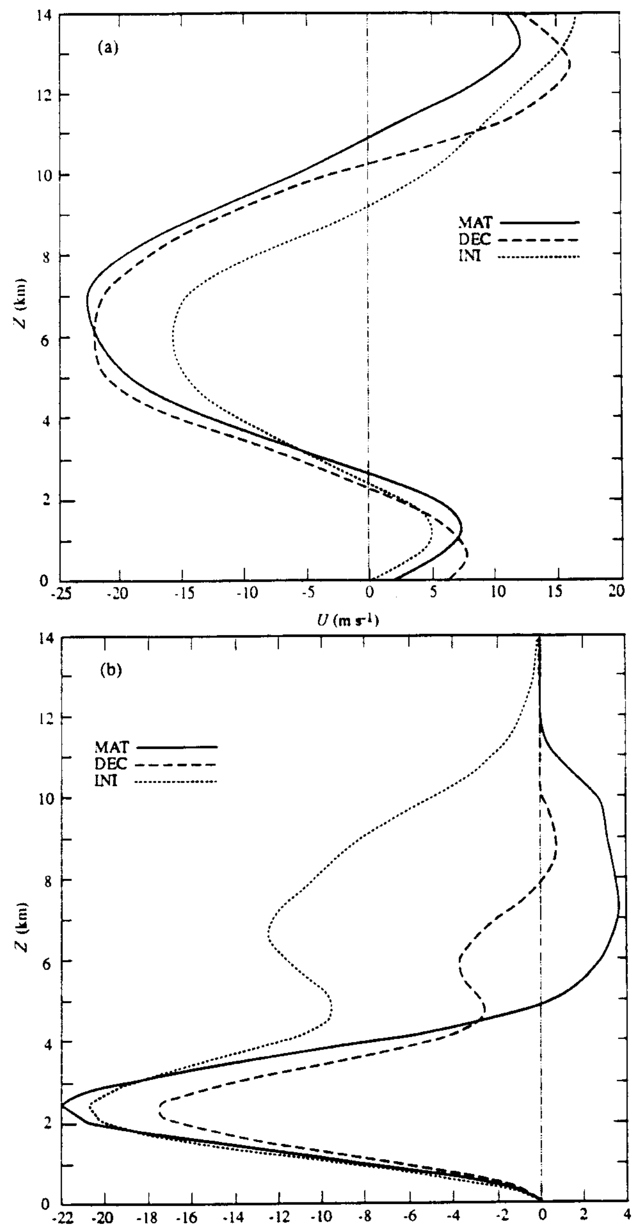

Fig. 4 The vertical profiles of the area-averaged horizontal wind (a) and momentum flux (b) in the convective region at three life cycle stages. INI denotes the initial stage, MAT the mature stage, and DEC the decaying stage, respectively.

gradient results in RTF acceleration within the whole troposphere except at low levels (below 2 km). Horizontal advection oscillates in the vertical but is again strongly out of phase with vertical advection. Sub-grid scale turbulence is again the smallest term. The net acceleration is FTR in upper and lower levels and RTF in between.

Initially, the momentum flux is mostly downgradient in the convective region, becomes more countergradient in the mature stage, and is mostly downgradient again in the decaying stage. However, in the stratiform region, the momentum transport is mostly countergradient initially, and becomes more and more downgradient as the system ages. The different momentum transport characteristics between convective and stratiform regions have not been addressed in previous studies. This will be our next phase of research.

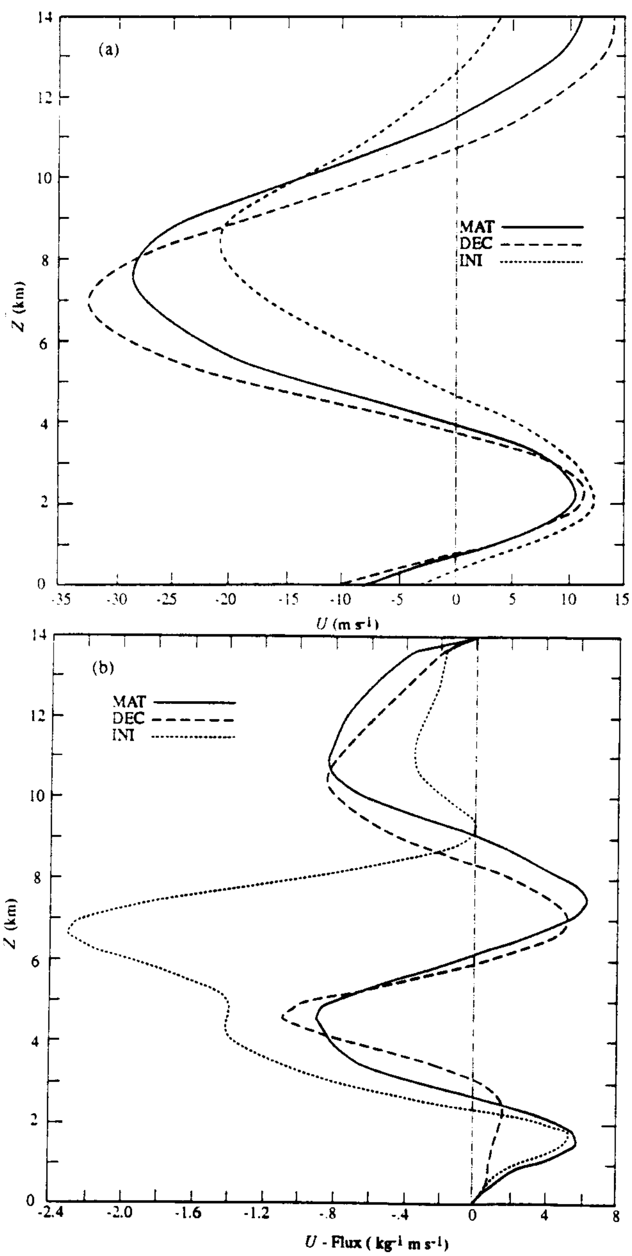

Fig. 5 The same as Fig. 4, except for the stratiform region.

Acknowledgments: The cooperation of Professor Robert G. Fovell has been vital to this study. G. C. Gudmundson edited the manuscript and K. M. Dewar assisted with the figures. The computations were made on the Cray Y-MP computer of the National Center for Supercomputing Application at the University of Illinois at Champaign-Urbana. This research was supported by the National Science Foundation grant ATM-9101653.

REFERENCES

Biggerstaff, M. I., and R. A. Houze, Jr., 1991: Kinematic and precipitation structure of the 10-11 June 1985 squall line. *Mon. Wea. Rev.*, **119**, 3034-3065.

Bluestein, H. B., and M. H. Jain, 1985: Formation of mesoscale lines of precipitation: Severe squall lines in Oklahoma during spring. *J. Atmos. Sci.*, **42**, 1711-1732.

Cunning, J. B., 1986: The Oklahoma-Kansas Preliminary Regional Experiment for STORM-Central. *Bull. Amer. Meteor. Soc.*, **67**, 1478-1486.

Fovell, R. G., and Y. Ogura, 1988: Numerical simulation of a midlatitude squall line in two dimensions. *J. Atmos. Sci.*, **45**, 3846-3879.

Fovell, R. G., and Y. Ogura, 1989: Effect of vertical wind shear on numerically simulated multicell storm structure. *J. Atmos. Sci.*, **46**, 3144-3176.

Gao, K., D.-L. Zhang, M. W. Moncrieff and H.-R. Cho, 1990: Mesoscale momentum budget in a midlatitude squall line: A numerical case study. *Mon. Wea. Rev.*, **118**, 1011-1028.

Houze, R. A., Jr., 1977: Structure and dynamics of a tropical squall-line system. *Mon. Wea. Rev.*, **105**, 1540-1567.

Johnson, R. H., and P. J. Hamilton, 1988: The relationship of surface pressure features to the precipitation and the air-flow structure of an intense midlatitude squall line. *Mon. Wea. Rev.*, **116**, 1444-1472.

Klemp, J. B., and R. B. Wilhelmson, 1978: The simulation of three-dimensional convective storm dynamics. *J. Atmos. Sci.*, **35**, 1070-1096.

LeMone, M. A., 1983: Momentum flux by a line of cumulonimbus. *J. Atmos. Sci.*, **40**, 1815-1834.

LeMone, M. A., G. M. Barnes and E. J. Zipser, 1984: Momentum flux by lines of cumulonimbus over tropic oceans. *J. Atmos. Sci.*, **40**, 1815-1834.

Lin, Y. L., R. D. Farley and H. D. Orville, 1983: Bulk parameterization of the snow field in a cloud model. *J. Climate Appl. Meteor.*, **22**, 1066-1092.

Smull, B. F., and R. A. Houze, 1985: A midlatitude squall line with a trailing region of stratiform rain: radar and satellite observations. *Mon. Wea. Rev.*, **113**, 117-133.

Zipser, E. J., 1969: The role of organized unsaturated convection downdrafts in the structure and rapid decay of an equatorial disturbance. *J. Appl. Meteor.*, **8**, 799-814.